A high-quality, homogenized, global, long-term (1993-2008) DORIS precipitable water data set for climate monitoring and model verification

Olivier Bock, Pascal Willis, Junhong Wang, Carl Mears

AGU PUBLICATIONS

JGR

Journal of Geophysical Research: Atmospheres

RESEARCH ARTICLE
10.1002/2013JD021124

Key Points:
- Sixteen years of global DORIS tropospheric delays are screened and homogenized
- DORIS precipitable water data are compared to GPS, radiosonde, and satellite data
- Precipitable water trends and variability are analyzed

Supporting Information:
- Readme
- Table S1
- Data Set S1

Correspondence to:
O. Bock,
Olivier.Bock@ign.fr

Citation:
Bock, O., P. Willis, J. Wang, and C. Mears (2014), A high-quality, homogenized, global, long-term (1993–2008) DORIS precipitable water data set for climate monitoring and model verification, *J. Geophys. Res. Atmos.*, *119*, 7209–7230, doi:10.1002/2013JD021124.

Received 31 OCT 2013
Accepted 8 MAY 2014
Accepted article online 16 MAY 2014
Published online 24 JUN 2014

A high-quality, homogenized, global, long-term (1993–2008) DORIS precipitable water data set for climate monitoring and model verification

Olivier Bock[1], Pascal Willis[2,3], Junhong Wang[4,5], and Carl Mears[6]

[1]IGN LAREG, University Paris Diderot, Sorbonne Paris Cité, Paris, France, [2]IGN DRE, Saint-Mandé, France, [3]IPGP UMR 7154 CNRS, University Paris Diderot, Sorbonne Paris Cité, Paris, France, [4]Department of Atmospheric and Environmental Sciences, State University of New York at Albany, Albany, New York, USA, [5]NCAR EOL, Boulder, Colorado, USA, [6]Remote Sensing Systems, Santa Rosa, California, USA

Abstract For the first time a high-quality, consistent, global, long-term data set of zenith tropospheric delay (ZTD) and precipitable water (PW) is produced from Doppler orbitography radiopositioning integrated by satellite (DORIS) measurements at 81 sites. The data set was screened using a two-level procedure. First, postprocessing information is used to apply range checks and outlier checks to ZTD and formal error estimates. Second, outliers are detected by comparing DORIS ZTD with European Centre for Medium-Range Weather Forecasts reanalysis (ERA-Interim) data. These procedures reject 3% and 1% of the data, respectively. A linear drift is evidenced in the screened DORIS ZTD data compared to ERA-Interim and Global Positioning System (GPS) data, which potentially results from biases introduced by the progressive replacement of Alcatel antennas with Starec antennas. The DORIS PW is homogenized by applying a bias correction computed form comparison with ERA-Interim data each time station equipment is changed. The homogenized DORIS data are in excellent agreement with GPS data (correlation of 0.98 and standard deviation of differences of 1.5 kg m^{-2}) and with ERA-Interim and satellite PW data (correlation $>$ 0.95 and standard deviation of differences $<$ 2.7 kg m^{-2}). The agreement with radiosonde data is less good. Preliminary results of water vapor trends and variability are shown for 31 sites with more than 10 years of data. Good consistency is found between DORIS PW trends and ERA-Interim trends, which demonstrates the high potential of the DORIS PW data set for climate monitoring and model verification. The final DORIS PW data set is freely available in the supporting information.

1. Introduction

Water vapor is a key ingredient of the global hydrologic cycle and plays an important role in many atmospheric processes contributing to the weather and climate [*Held and Soden*, 2000; *Solomon et al.*, 2007]. Monitoring accurately the water vapor trends and variability at all pertinent scales is a challenging task which requires the combination of various types of observations (e.g., sensing the lower and the upper atmosphere) with global coverage. Ground-based networks and long-term satellite missions play a crucial role in this task. Humidity measurements in the troposphere have been made since the 1950s using radiosonde balloons equipped with pressure, temperature, and humidity sensors. But the global radiosonde data record covers mostly the Northern Hemisphere, and its usefulness for climate monitoring is limited by errors and biases associated with the instruments and by discontinuities due to changes in sensors and procedures over time [*Ross and Elliott*, 2001; *Wang et al.*, 2001; *Trenberth et al.*, 2005; *Dai et al.*, 2011]. Total column water vapor and profiles of tropospheric humidity have been measured by satellites since the end of the 1970s, but long-term trends are difficult to derive from satellite data because of intercalibration limitations [*Mieruch et al.*, 2008; *Shi and Bates*, 2011]. The ground-based Global Positioning System (GPS) is presently one of the most reliable technique for sensing precipitable water (PW) with accuracy at the level of 1–2 kg m^{-2} or 5% in all weather conditions [*Bock et al.*, 2007; *Wang et al.*, 2007; *Byun and Bar-Server*, 2009]. The International Global Navigation Satellites System Service (IGS) operates a global GPS network of ~400 stations among which about 100 have data extending back to 1995 [*Dow et al.*, 2009]. GPS PW has been used for detecting humidity biases in radiosonde data and numerical weather prediction models [*Wang and Zhang*, 2008; *Bock and Nuret*, 2009; *Wang et al.*, 2013] and for studying atmospheric processes and climate trends [*Bock et al.*, 2008; *Nilsson and Elgered*, 2008; *Wang and Zhang*, 2009; *Ning and Elgered*, 2012]. However, changes in instrumentation and processing options have been shown to produce shifts in the long time series which

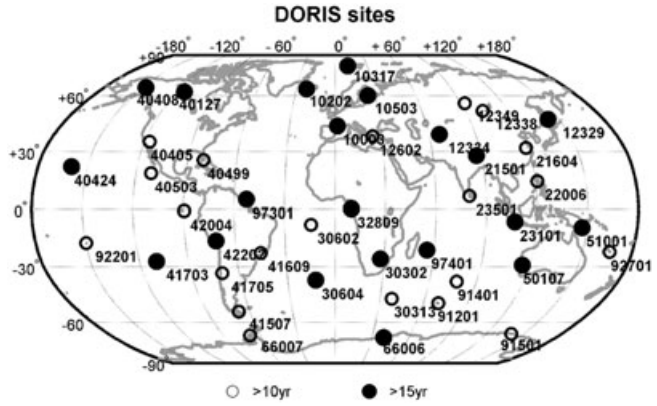

Figure 1. Map showing the locations of DORIS sites and duration of observations used in this study (information from http://www.ipgp.fr/~willis/DPOD2008/DPOD2008_1.11.txt). There are 42 sites with more than 10 years and less than 15 years of data and 21 sites with more than 15 years, between 01 January 1993 and 23 August 2008. The historical DORIS data cover the period from 1990 to present, for which 27 sites have more than 20 years of data.

require special data postprocessing before trends can be estimated from this data set [*Vey et al*., 2009; *Bock et al*., 2010].

DORIS (Doppler orbitography radiopositioning integrated by satellite) is a satellite tracking system primarily used for positioning low Earth-orbiting satellites, initially for altimeter missions and later used for geodetic and geophysical applications in complement to GPS [*Willis et al*., 2006]. It is in operation since January 1990 and is composed of a network of about 60 ground transmitters homogeneously distributed around the globe (Figure 1). Satellites equipped with DORIS receivers collect the signals transmitted by the ground-based beacons either for processing their orbits in realtime [*Jayles et al*., 2010] or in view of getting accurate postprocessed orbits such as required, e.g., by altimetry mission satellites [*Lemoine et al*., 2010]. Postprocessing in geodetic mode also allows retrieving station positions and tropospheric delays using a very similar approach as for GPS measurements [*Le Bail et al*., 2010; *Stepanek et al*., 2010; *Willis et al*., 2010a]. The DORIS data and products are freely available at the International DORIS Service (IDS) data centers [*Tavernier et al*., 2002; *Willis et al*., 2010b]. In a recent study, we compared DORIS zenith tropospheric delay (ZTD) data with GPS ZTD data over a 4 year period [*Bock et al*., 2010]. We found an overall good agreement, though DORIS showed a significantly larger random scatter than GPS primarily because of fewer observations (there are only from 2 to 6 DORIS-equipped satellites at a time compared to 24 to 30 GPS satellites, see Figure 2b and Table 1). The standard deviation of DORIS minus GPS ZTD differences was 8.6 mm for high-resolution data and 2.4 mm for

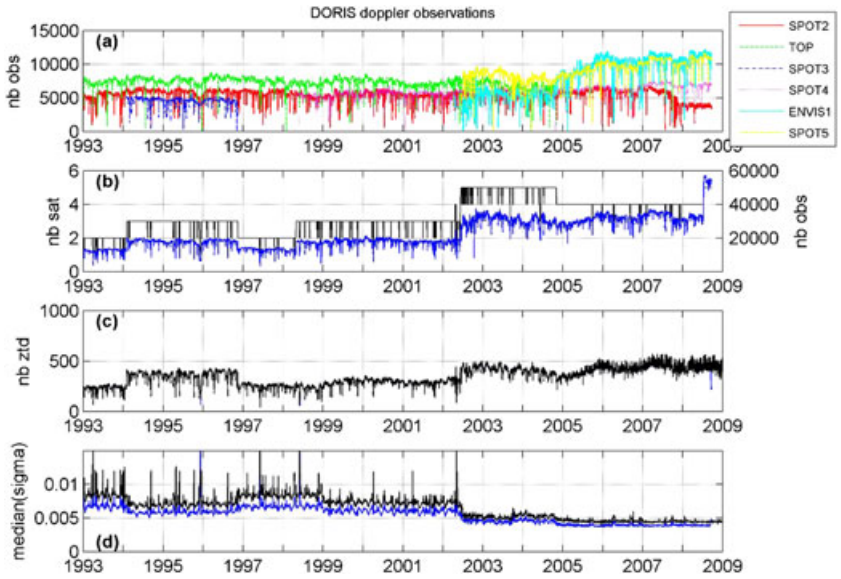

Figure 2. (a) Time series of the daily number of Doppler observations collected by each satellite; (b) number of available satellites (black, left scale) and total number of Doppler observations (blue, right scale); (c) total number of ZTD estimates (all stations together) for a solution with fixed position (blue) and estimated position (black); (d) median formal error of ZTD estimates (over all stations) for fixed (blue) and estimated position (black).

Table 1. DORIS Data Availability at the IDS Data Centers (From January 1993 to December 2012), Sorted by Time of First Observation[a]

Satellite	Altitude (km)	Inclination	Start	End	Mission Objective
SPOT-2	830	98.7°	1 Jan 1993	14 Jul 2009	remote sensing
TOPEX/Poseidon	1330	66°	1 Jan 1993	18 Jan 2006	altimetry
SPOT-3	830	98.7°	1 Feb 1994	13 Nov 1996	remote sensing
SPOT-4	830	98.7°	1 May 1998	…	remote sensing
Jason-1	1330	66°	15 Jan 2002	…	altimetry
Envisat	800	98.6°	10 Apr 2002	08 Apr 2012	altimetry/environment
SPOT-5	830	98.7°	11 Jun 2002	…	altimetry
Jason-2	1330	66°	12 Jul 2008	…	remote sensing
Cryosat-2	720	92°	30 May 2010	…	altimetry/cryosphere
HY-2A	970	99.4°	1 OCT 2011	…	altimetry

[a]Active satellites at the end of this period are noted as "…". Note that the present study uses only data between 01 January 1993 and 23 August 2008.

data smoothed with a 5 day moving average. DORIS appeared as a useful technique for monitoring PW at timescales longer than a few days in complement to GPS and other ground-based techniques. The long history (more than 20 years) makes it especially relevant for trend analysis.

The goal of this study is to (1) develop a methodology for screening and homogenizing the long-term DORIS ZTD data; (2) apply this methodology to produce a high-quality consistent global DORIS ZTD and PW data set back to January 1993; (3) validate the DORIS ZTD and PW estimates by comparison with independent data sets; (4) provide some preliminary highlights of water vapor trends and variability. The data set developed in this work is made available to the scientific community in the supporting information. The processing and postprocessing of DORIS measurements and the characteristics of the various data sets are introduced in section 2. The methodology for screening and homogenizing the DORIS ZTD data is developed and assessed in section 3. The screening consists of a two-level procedure. The first level is based on the use of postprocessing information and on the application of range checks and outlier checks on DORIS ZTD and formal errors. The second level relies on the comparison of DORIS ZTD data with European Centre for Medium-Range Weather Forecasts (ECMWF) reanalysis (ERA-Interim) ZTD data. The screened DORIS ZTD data set is validated with additional comparisons with GPS ZTD data. Inhomogeneity in the DORIS ZTD time series is detected from the ZTD comparisons and is corrected using constant piecewise bias estimates. Section 4 presents the comparisons of DORIS PW data with four independent PW data sets (ERA-Interim, GPS, radiosondes, and satellites). Preliminary highlights of water vapor trends and variability are also presented. Conclusions and perspectives are given in section 5.

2. Data and Methods

2.1. DORIS Measurements and Data Processing

The DORIS Doppler observations were processed using GIPSY-OASIS II software package [*Zumberge et al.*, 1997] with the same strategy as the one used by *Bock et al.* [2010] but over a longer period of time (January 1993 to August 2008). Compared to previous releases, this strategy (referred to as ignwd08) [*Willis et al.*, 2012b] uses an improved method for mitigating errors in solar radiation pressure models [*Gobinddass et al.*, 2009] and atmospheric drag corrections [*Gobinddass et al.*, 2010]. The data were processed on a daily basis. Two solutions were produced: one with station positions estimated simultaneously with zenith wet delay (ZWD) parameters and the other with positions fixed at the reference frame solution determined by *Willis et al.* [2010b] (referred to as tf_090123). The ZWDs were estimated per station, at start of satellite passes and at a frequency of less than 20 min (see more details in *Bock et al.* [2010]). ZWDs were only estimated when DORIS measurements were available for a given ground station and a given satellite. It must be noted that, unlike what is done by other DORIS analysis groups, the DORIS data in this study are processed at observation level in a multisatellite mode and the estimated ZWD parameters are consequently only station-dependent and not satellite-dependent. Other estimated parameters were orbit elements and empirical accelerations (once-per-revolution along-track and cross-track accelerations), clocks drifts for ground stations and all satellites but one (used as time reference).

The tropospheric delay was modeled a priori with a standard formula for the hydrostatic component, based on standard sea level surface pressure extrapolated as a function of altitude [*Zumberge et al*., 1997]. The global mapping function (GMF) [*Boehm et al*., 2006] was used for the projection of zenith tropospheric delay into the direction of DORIS satellites. The cutoff angle was set to 10°. Several variants of tropospheric delay modeling were tested, such as estimating horizontal tropospheric gradient parameters to take into account the local asymmetries of the troposphere [*Willis et al*., 2012a], but the results were not significantly different from those presented here (without gradients estimated). The processing outputs of interest here are ZTD estimates and their formal error estimates. As a basic principle with least squares and Kalman filtering methods, the formal error depends on the satellite geometry, on the number of estimated parameters, on the number of observations, and is scaled by the assumed uncertainty in the Doppler observations (e.g., 0.5 mm s^{-1}) [*Williams and Willis*, 2006]. The number of observations is conditioned by the number of available DORIS satellites and by the station's latitude (stations at higher latitudes generate more observations with Sun-synchronous satellites). Table 1 lists the available satellites for the period of study. Figure 2d shows the time series of formal errors. When a new satellite becomes available (e.g., SPOT3 in 1994 or SPOT4 in 1998) the number of observations (Figure 2b) and the number of estimated ZTDs (Figure 2c) increase and simultaneously the formal error decreases (Figure 2d). For any given station, one can verify that the formal error roughly decreases as $N_{obs}^{-1/2}$ (as predictable using a white noise assumption). The formal error also depends on the quality of the observations, which is not the same for all the satellites as receiver technology has significantly improved since 1990 [*Auriol and Tourain*, 2010]. Figure 2d reveals a significant reduction of formal error by mid-2002 following the addition of SPOT5 and ENVISAT satellites. Another smaller reduction is also seen at the end of 2004 coincident with the stop of TOPEX satellite and an increase in the number of observations collected by the SPOT5 and ENVISAT satellites. Figure 2d also compares two DORIS solutions, one with station positions estimated (free-network solution) and one with positions fixed. Fixing the positions to reference values reduces the number of parameters in the least squares problem and consequently diminishes the magnitude of the formal errors (compare blue and black curves in Figure 2d). It also stabilizes the numerical procedure by eliminating the correlation between ZTD, station height, and ground station clock parameters. However, if positions are fixed, errors from geophysical site displacements propagate into ZTD because station positions are fixed. Compared to GPS data analysis, where it is more of a standard to simultaneously estimate station coordinates and ZTD parameters in daily sessions, for DORIS, due its technical specificity (2 to 6 satellites instead of about 30 for GPS), the daily station position cannot be determined better than within 2 or even 3 cm (instead of 3–6 mm for GPS). It is thus more accurate to use a long-term DORIS solution which can be provided with a precision better than 1 cm for any day during the observation period. We analyzed both solutions but we will mainly present here the solution with fixed positions as it provided more accurate results.

For Precise Orbit Determination (POD) applications, the metadata identifying the periods at each station, for which the DORIS Doppler observations may not be considered reliable, are also available since the beginning of the DORIS observations [*Willis and Ries*, 2005]. These periods correspond typically to geophysical events (nearby Earthquake or volcanic activity), or ground equipment technical issues (antenna instability, insufficient stabilization of internal clock, etc.). This kind of information is referred to as DORIS-POD (DPOD) metadata and is available online at http://www.ipgp.fr/~willis/DPOD2008/. The DPOD2008 metadata used in this study represent the most recent update of DPOD2005 [*Willis et al*., 2009] based on International Terrestrial Reference France (ITRF) 2008 realization, ITRF2008 [*Altamimi et al*., 2011].

In the following we will distinguish between DORIS sites, identified by the first five digits of the station DOMES numbers (http://itrf.ensg.ign.fr/domes_desc.php), and DORIS stations identified by a four-character identifier usually derived from the station location (e.g., ADEA for Terre Adelie, Antarctica). As a rule at IDS, DORIS station names are changed when the instrumentation onsite is changed or relocated. In the DORIS naming convention, the last character identifies the antenna type. It can either be A for Alcatel antennas used for the initial set up of the network or B for Starec antennas which replaced the former progressively as the system was upgraded. The changes other than antenna replacement are reflected in the third character. For example, station ADEA attached to site 91501 became ADEB on 1 January 2002 when the antenna was changed and ADFB on 8 February 2008 when antenna support was raised by 40 cm (http://ids-doris.org/network/sitelogs.html). Over the period of study, there are 150 stations located at 81 sites, but

only 146 stations located at 79 sites were used because the others did not have precise coordinate estimates available at the time of processing (see section 3.1).

2.2. ECMWF Reanalysis

The ECMWF reanalysis, ERA-Interim, is the most recent global long-term atmospheric reanalysis produced by ECMWF [*Simmons et al*., 2006]. It extends back to 1979. Mean sea level pressure, 2 m temperature and dew point, and PW were retrieved on a regular grid with a $0.75° \times 0.75°$ horizontal resolution and 6 h time interval for the period 1993.0–2009.0. For the conversion of DORIS ZTD to PW and the comparison with DORIS ZTD and PW data, ERA-Interim data from the four grid points surrounding each DORIS station are interpolated vertically and horizontally following the procedure described in *Bock et al*. [2007]. The standard deviation of the ZTD values over the four grid points surrounding the DORIS station after the vertical interpolation reflects the spatial variability of ZTD and can be used as a measure of the representativeness difference between the DORIS data and the reanalysis data. For 90% of the stations, the median value of this standard deviation is smaller than 0.025 m. The largest values reach 0.17 m and are found for stations in mountainous areas where the representativeness difference is expected to be increased. Indeed, at 33 stations out of 146, one of the four surrounding model grid points has a difference in elevation of more than 500 m with respect to the DORIS station. These stations were eventually blacklisted because representativeness differences in the reanalysis data are likely to introduce errors in the surface pressure data used to convert DORIS and GPS ZTD to PW as well as in the PW intercomparisons. For the intercomparisons, the DORIS and ERA-Interim data are matched in time within ± 3 h. Since the reanalysis values are representative of the specified epoch, they are matched with the temporally closest DORIS values. Each DORIS or model value is used only once in the comparison to avoid the introduction of artificial serial correlation in the results. Previous studies evaluating PW data from ECMWF analysis and reanalysis to independent GPS PW estimates found biases at given stations in the range -3.0 to $+3.4\,\mathrm{kg\,m^{-2}}$ in Africa [*Bock et al*., 2007; *Bock and Nuret*, 2009] and -1.2 to $+1.2\,\mathrm{kg\,m^{-2}}$ in Europe [*Ning et al*., 2013], but the mean biases over these regions were usually smaller than $0.5\,\mathrm{kg\,m^{-2}}$.

2.3. Reprocessed GPS ZTD Solution From IGS

The GPS ZTD solution used in this study is a reprocessing of the operational IGS tropospheric product [*Byun and Bar-Server*, 2009] produced by Jet Propulsion Laboratory in 2010 [*IGSMAIL-6298*, 2012] and is available for the period 1 January 1995 to 31 December 2007. Thanks to the use of most recent tropospheric models [*Boehm et al*., 2006], absolute antenna models [*Schmid et al*., 2007], and IGS05 reference frame [*Ferland and Piraszewski*, 2009], the accuracy of this GPS ZTD data set is expected to be higher than all the previous releases provided by IGS. The use of a fixed strategy for processing the complete data set also guarantees a high level of homogeneity. The GPS PW data has been validated in many past studies [e.g., *Bock et al*., 2007; *Wang et al*., 2007; *Byun and Bar-Server*, 2009, and references therein]. However, the accuracy of GPS PW data is still subject of on-going research because it depends on the way the data are processed (e.g., *Ning and Elgered* [2012] for an evaluation of changes in bias as a function of cutoff angle) and the ZTD is converted to PW [*Ning et al*., 2013], as well on error sources specific to each instrument and site [*Bock et al*., 2013].

The DORIS and GPS stations are paired according to the first five digits of their DOMES numbers (same country and city or province). We found 96 pairs of stations with data available for the period of study (1995.0–2008.0). The largest difference in elevation between DORIS and GPS stations is 172 m and the largest distance is 30 km. Only six pairs have actually a difference in elevation larger than 100 m. For the comparison with DORIS data, the GPS data were corrected for the effect of the difference in station elevations following the method described by *Bock et al*. [2010] and using atmospheric surface parameters extracted from ERA-Interim. The GPS ZTD estimates are available with a 5 min time interval and are matched with the DORIS data within ± 1.1 h.

2.4. Radiosonde PW Data

Global radiosonde humidity data represent an important resource for understanding atmospheric processes and monitoring climate change. Unfortunately, the application of radiosonde humidity measurements in climate studies is hampered by sensor-dependent errors that changed significantly over time and space [*Wang and Zhang*, 2008]. A new approach to homogenize the daily radiosonde humidity data was recently proposed by *Dai et al*. [2011]. This method allows mapping the statistical properties of the most recent and

accurate radiosonde measurements to the older ones and provides hence a means to remove the overall biases in the distributions of radiosonde humidity data. This approach was combined with a new radiation dry bias correction method that applies to the most recent Vaisala RS92 measurements to achieve a corrected homogenized radiosonde data set that is used in the present study. This correction is able to reduce the radiosonde PW bias compared to GPS PW to $\pm 0.5\ \mathrm{kg\,m^{-2}}$ on average and to reduce its dependence upon the total PW and its diurnal cycle [*Wang et al*., 2013].

DORIS sites are matched with radiosonde sites with thresholds of 50 km, 100 m, and 1 h for horizontal, vertical, and temporal separations, respectively. The matching selected 54 DORIS stations at 38 DORIS sites. For the comparison with DORIS data, no vertical adjustment is applied as the altitude difference is here limited to ±100 m. The radiosonde data are available at 00 UTC and/or 12 UTC and are matched with the DORIS data within ± 3 h.

2.5. Microwave Radiometer Satellites

We used PW data from Special Sensor Microwave Imager (SSM/I) and from the Special Sensor Microwave Imager Sounder (SSMIS) on board seven of the Defense Meteorological Satellite Program (DMSP) satellites (F10, F11, F13, F14, F15, F16, and F17) and from the Advanced Microwave Scanning Radiometer-Earth (AMSR-E) Observing System Sensor on board the NASA Aqua Satellite. The PW estimates from these instruments were produced at Remote Sensing Systems [*Wentz*, 2013]. The uncertainty in the final gridded PW data can be evaluated by propagating the estimated errors in satellite measured brightness temperatures, observing angle and ancillary data that is input to the algorithm (sea surface temperature and wind direction) through the algorithm. The estimated uncertainty depends on PW, starting at $0.3\ \mathrm{kg\,m^{-2}}$ for low values of PW and increasing to $0.6\ \mathrm{kg\,m^{-2}}$ for values above $60\ \mathrm{kg\,m^{-2}}$. This should be thought of as a lower limit of the uncertainty, as it does not contain possible algorithm biases. Comparisons with ground-based GPS and microwave radiometer PW data on islands and coastal areas found station-dependent biases in the range -2.4 to $0.7\ \mathrm{kg\,m^{-2}}$ for Africa [*Bock et al*., 2007] and $-0.5\ \mathrm{kg\,m^{-2}}$ in the western South Pacific [*Lindstrot et al*., 2014]. While the cause of these biases is not known, they likely arise from a combination of biases in the GPS data, biases in the satellite data, and biases due to spatial mismatch between the point-like GPS measurement and the spatially extended microwave measurements.

The data from these instruments intersect the DORIS data for various periods: 1993–1997 (F10), 1993–2000 (F11), 1995–2009 (F13), 1997–2009 (F14), 1999–2008 (F15), 2003–2008 (F16), 2006–2008 (F17), and 2002–2008 (AMSR-E). Hereafter, the PW data from the SSM/I, SSMIS, and AMSR-E instruments will be referred to all together as satellite data.

Only coastal and island DORIS stations are considered as the satellite data are available only over the oceans. The matching selected 20 stations located at 12 sites. The satellite data are extracted from the gridded daily data sets provided by RSS by evaluating a five by five set of gridded cells centered on the stations. Here we use the average over the portions of the 25 footprints that contain valid satellite data. Satellite data are often missing near each station due to the presence of land. The satellite data quality assurance uses a land mask to remove any grid points that are contaminated by the presence of land. This land mask is intended to be very conservative and no bias as a function of distance from land could be evidenced. For the DORIS versus satellite comparison, the DORIS PW is adjusted to the mean sea level. The time series from DORIS and satellites are matched in time within ± 3 h.

2.6. ZTD/PW Conversions and Comparisons

The conversion of DORIS and GPS ZTD to PW, and the conversion of ERA-Interim PW to ZTD, are performed using the following formulas: ZTD = ZHD + ZWD and PW = ZWD/ K(T_m), where ZHD is the hydrostatic zenith delay computed from the ERA-Interim surface pressure and K is a function of the mean temperature, T_m (see *Bock et al*. [2007] or *Wang and Zhang* [2009] for further details). The T_m data were extracted from the Technical University of Vienna database (http://ggosatm.hg.tuwien.ac.at/DELAY/ETC/TMEAN/). These T_m estimates are computed from ERA40 reanalysis before 2002 and ECMWF operational analysis after 2002 from pressure level data starting using the same topography which ensures that the T_m product is consistent over time (J. Boehm, personal communication, 2013). Moreoyer these T_m estimates are also consistent with the ERA-Interim surface data. The horizontal interpolations and adjustments of surface pressure and

PW for difference in DORIS and GPS station heights are computed following the method described in *Bock et al*. [2007].

Several statistical parameters are computed from the following matched time series: mean and standard deviation of differences, linear correlation coefficient, and linear regression line. The linear regression line is computed assuming errors in both variables [*York et al*., 2004]. For DORIS and GPS we use the formal errors (see section 2.1) as error estimates to compute the linear regression line. For ERA-Interim, we use the standard deviation of the ZTD values over the four grid points surrounding the DORIS station measure of the representativeness difference between the DORIS data and the reanalysis data. For the radiosonde we used a 10% fractional error on PW and for the satellite data 5% on PW, based on previous studies [*Bock et al*., 2007; *Mears et al*., 2007; *Wang et al*., 2007]. Note that compared to the traditional linear regression method with errors only in one variable, the method assuming errors in both variables usually provides larger values for the slope parameter (i.e., slope is more often above 1).

3. Screening and Homogenization of DORIS ZTD Data

The accuracy of ZTD values estimated from the processing of Doppler data (section 2.1) depends on many factors and is usually time and station dependent. In order to keep the best values for each station, an adaptive screening has to be applied to reject outliers and less accurate values and a homogenization method has to be applied to remove the discontinuities due to instrumental changes. Since there is no standard method established yet for the screening and homogenization of ZTD data, we propose those described in the following section. The proposed tests and thresholds were determined after several trials and are adapted to the present data set.

3.1. Screening Based on the Analysis of DORIS Postprocessing Data

A screening method is developed for the rejection bad DORIS ZTD data. It is based on the use of information contained in the DPOD metadata files and on a quality check applied to ZTD values and to the formal errors of the ZTD values. The algorithm comprises seven tests listed below which are applied sequentially to the data for each station (i.e., only the data that pass a test are transferred to next test), independently for each station and each year:

1. Station rejection: reject all data from station if coordinates are not fixed (postprocessing information).
2. DPOD blacklisting: reject data for periods flagged as "bad" in the DPOD metadata.
3. Station rejection: reject all data from station if the median formal error exceeds 0.02 m.
4. ZTD range check: reject data for which ZTD is outside the interval [0; 3 m].
5. Formal error range check: reject data for which formal error is larger than 0.03 m.
6. ZTD outlier check: reject data for which ZTD is outside the interval [median(ZTD) − 0.5 m; median(ZTD) + 0.5 m].
7. Formal error outlier check: reject data if formal error is outside the interval [0.001 m; med(ε) + 3 std(ε)] where med(ε) and std(ε) are the median and the standard deviation of formal error.

Test # 1 was introduced because it appeared that for a small number of the stations precise coordinates were not known when this data set was processed. This was the case for CARB, OTT2, WAIA, and MSOB, which were new stations or stations deployed for a short period of time (e.g., during field campaigns). The coordinates of these stations were estimated during the processing, whereas they were fixed for the other stations. In order not to mix data with fixed and estimated coordinates, the data from these four stations were rejected.

Test # 2 uses the metadata from the DPOD file to reject data flagged as bad by the IDS analysis centers during operational analysis. This test rejects a significant number of data (Figure 5, later).

Test # 3 rejects all data from a station if the yearly median formal error exceeds a threshold of 0.02 m. This level was chosen after inspection of the yearly formal error statistics for all stations and all years. Figure 3a gives an overview of the initial distributions of formal error, based on percentiles, for all stations in 1993. Note that we use percentiles instead of mean and standard deviation because the latter statistics are not adapted to represent non-Gaussian distribution (Figure 4b, later). The median formal error (black curve) exhibits some scatter from one station to another, but all except three stations have a median below 0.015 m.

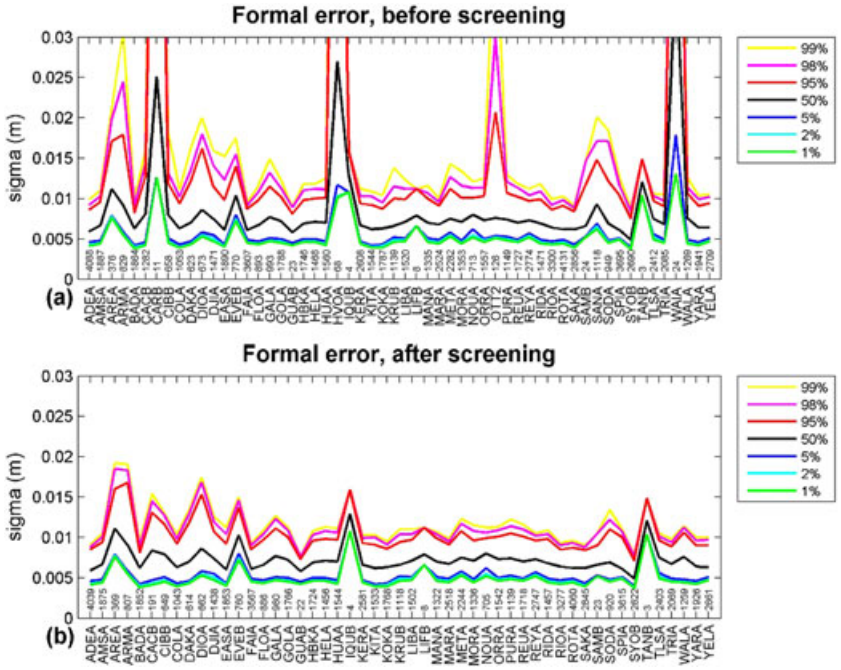

Figure 3. Percentiles of formal error (sigma) of DORIS ZTD estimates for all stations in 1993; (a) before and (b) after data screening. The lines represent the 99th, 98th, 95th, 50th, 5th, 2nd, and 1st percentiles from top to bottom, respectively (the black line shows the median). Station names and number of data points (ZTD estimates) are indicated at the bottom of each plot.

These three stations are CARB, HVOA, and WAIA, which do not have fixed coordinates and are in fact rejected by test # 1. When applied to all 16 years of the study, only two stations are rejected by this test: HVOA in 1993 and ASDB in 1997.

Tests #4 to 7 are applied to each data point of the yearly time series. The range check limits in tests (4) and (5) are very broad and are the same for all the stations. The outlier check limits are computed from the median and standard deviation of the data and match the statistical properties of each station. It is useful to preselect the data with the range checks before computing the outlier check limits because the standard deviation is not a robust estimator. Figure 3b shows the distributions of formal error after all seven screening

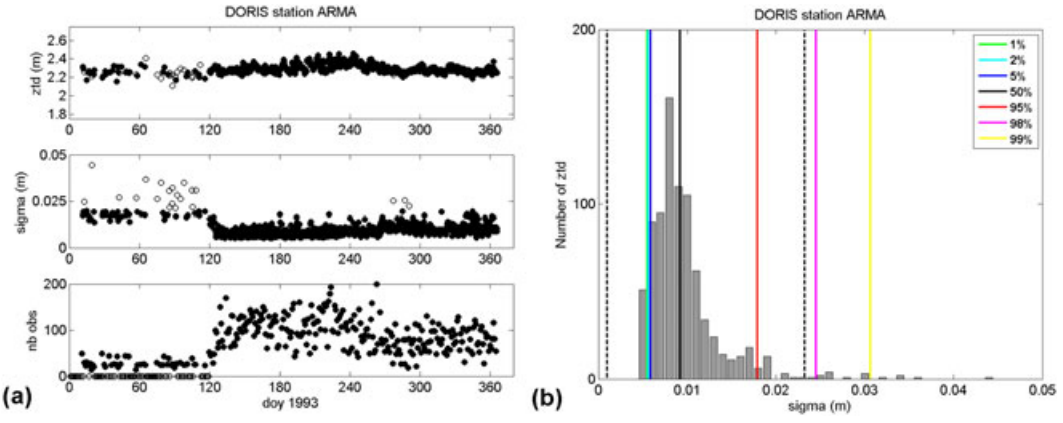

Figure 4. (a) Time series of high-resolution ZTD, formal error (sigma) and daily number of Doppler observations for station ARMA in 1993. No ZTD is estimated when the number of observations is zero. The open symbols show the points that are rejected during the data screening. (b) Histogram of formal errors for station ARMA in 1993. The solid vertical lines show the 1st to 99th percentiles as indicated in the legend (the dashed line shows the median). The black dotted vertical lines show the outlier check limits (0.001 m and median + 3 standard deviations).

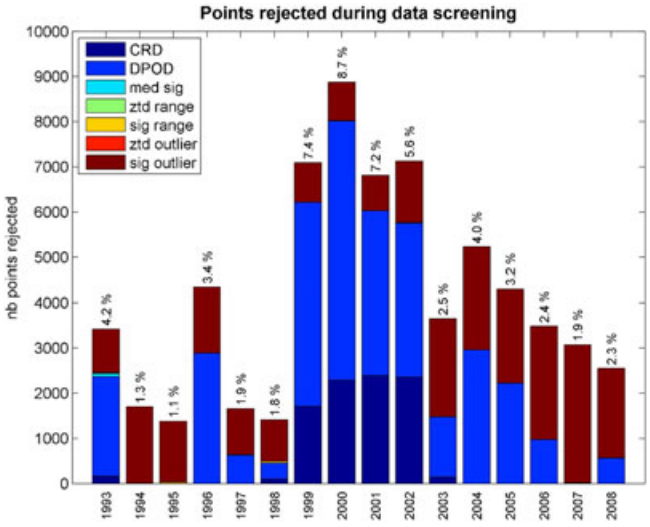

Figure 5. Number and fraction of data points rejected by each of the seven tests of the first screening level for each year (see section 3.1). The number of points rejected by each test is 9,137 for CRD, 78 for med sig, 31,390 for DPOD, 7 for ZTD range, 136 for sigma range, 3 for ZTD outlier, and 25,397 for sigma outlier. The total number of points rejected is 66,148 and the total number of points available after the screening is 1,878,949. The second screening level, based on ZTD comparison with ERA-Interim rejects additionally from 0.9 to 1.3%.

tests are applied to the data from 1993. Apart from the three stations that are rejected, the main impact is seen on the 99th and 98th percentiles for most stations. This results from the choice of the upper threshold of the formal error outlier check (test #7).

Figure 4a illustrates the temporal variations of ZTD values and associated formal errors for station ARMA. It is generally difficult to detect the spurious values in the ZTD series without use of a reference ZTD series (this is the purpose of the second-level screening). The formal errors, on the other hand, show strong variations. Large values of formal error are associated with small numbers of Doppler observations. Figure 4b shows the histogram of formal errors. The upper threshold of 3 standard deviations used in test #7 cuts the tail of the histogram just below the 98th percentile hence rejecting slightly more than 2% of data.

Figure 3b shows that after the screening, all the stations have more symmetrical distributions around the median and that stations with large medians generally show also large values in the higher percentiles (95th – 99th). A few stations still have large median values and should either be rejected (e.g., IQUB and TANB) or regarded with caution in the following (AREA, EVEB, ARMA, DIOA, CACB, and SODA).

Figure 5 shows the number of data points rejected for each year and for each of the seven screening tests. Test #2 and #7 are those that reject most of the data. Test #2 rejects data from 16 stations which have temporary problems, especially over the period 1999–2002, but the reason for this is not explained yet. Test #7 rejects a quite large number of data every year but there is a clear increase in the number of data rejected in 2003 and later. This increase is explained by a significant change in position and width of the probability density function (PDF) of formal error in 2003 that follows from the increase in the number of observations (Figure 2b). The empirical PDF of formal error follows a noncentral $\chi 2$ PDF (Figure 4b) with a degree of freedom comprised between 11 in 1993 and 4 in 2003 and later. As the degree of freedom decreases, the PDF shifts to the left but the median plus three standard deviations limit shifts quicker than the high percentiles. Hence, a larger fraction of data is rejected from test #7 when the data become more accurate after 2003. However, the number of data rejected remains acceptable. Overall, test #2 and #7 together reject 3.0% of the data points and all tests together reject 3.5% of the data points. Among the 150 stations initially available, 144 are left after the screening. The stations rejected are as follows: CARB, OTT2, WAIA, MSOB, AMSB, and HVOA.

3.2. Screening Based on the Comparison of DORIS and ERA-Interim ZTD Data

It appeared useful to complement the screening with a more physical screening based on the comparison of the DORIS ZTD data with a reference ZTD series. Because the reference should be homogeneous in space and time and available for all the stations, we use a reanalysis. A reanalysis product is generated by a constant state-of-the-art numerical data assimilation technique using various past observations. Therefore, it less likely contains spurious outliers and can be used as a reference.

The first step consists in forming ZTD differences (DORIS minus ERA-Interim) for each station and each year. The test then consists in rejecting the data points corresponding to the ZTD differences that do not match normality. Indeed, for a Gaussian PDF, only 0.27% of the values should fall outside the mean ± 3

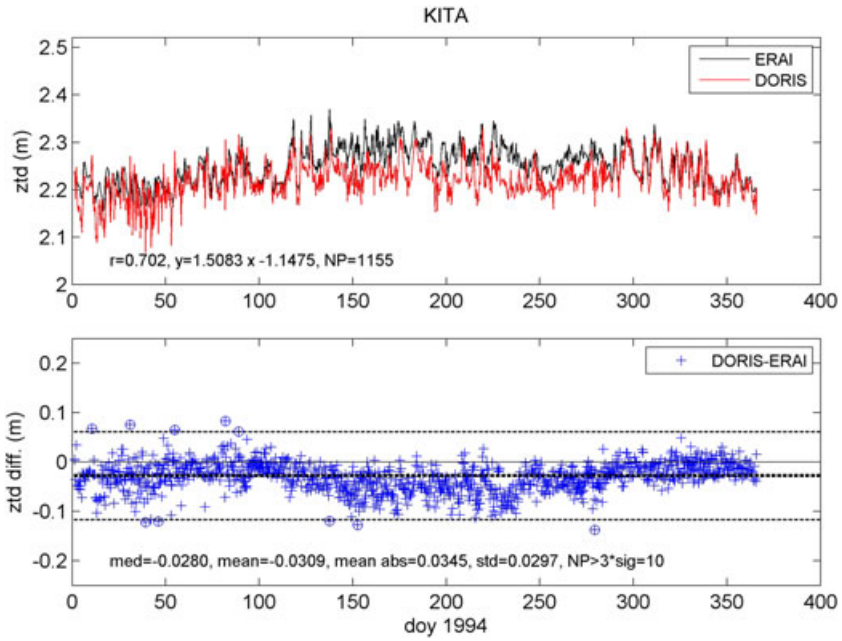

Figure 6. Time series of matched DORIS and ERA-Interim ZTD data and their differences for station KITA (Kitab, Uzbekistan) in 1994. The circles in the difference plots identify points that are beyond the median ± 3 times the standard deviation limits.

standard deviations interval. If there are more values outside this interval, it is probable that these contain outliers and the test will reject these values. Given that the empirical PDF is not perfectly Gaussian, we relax the constraint and allow up to 0.54% of the values to fall outside the above range limits. Moreover, since the mean and standard deviation are not robust estimators, we use the median instead of the mean and the half distance between the 16th and 84th percentiles instead of the standard deviation. This test is applied recursively and the detected outliers are removed at each pass. The iterations stop when there are no more outliers detected or 10 iterations are reached. Practically, the largest number of iterations was seven, so the test always converged, and the largest number of points rejected for a station was 88 for a single year. Overall, only 0.95% of the data are rejected with this test.

The ZTD difference observed at most stations appeared random and stationary, with a nearly Gaussian PDF. Only a few stations did not follow this behavior. Figure 6 shows such an example. Station KITA (Kitab, Uzbekistan) shows a seasonal signal in ZTD difference which is due to systematically smaller DORIS ZTD data in summer (day 120 to 250) compared to ERA-Interim. This feature is observed every year independently of the change of antenna and beacons and seems attached to the site rather than to the DORIS equipment. This seasonal effect could be due to the seasonal cycle of the nearby vegetation, as already clearly demonstrated for station JIUB (Jiufeng, China) by *Ferrage et al*. [2012] or to a representativeness difference between the DORIS ZTD data and the model data due to the elevation difference between the station and nearest reanalysis grid point (510 m). We suspect this is the case for a small number of other sites (AREA, EVEB, KOKA, MORA, and SANA). However, the representativeness difference is expected to be stationary and thus changes in the comparison results can be used to detect discontinuities in the quality of the DORIS measurements.

Table 2 presents the statistics of yearly DORIS-ERA-Interim comparisons applied to the data that passed both screening level. There are 866 comparisons produced from the 144 stations and 16 years. The median values reflect overall very good agreement between the two data sets, with a small bias (−0.004 m), small standard deviation (0.017 m), and high temporal correlation (0.93). But the dispersion in the results is quite large, as reflected in the minimum/maximum range and 5th–95th percentile interval. Because representativeness differences can limit the comparisons, we selected a subset of comparisons for which the elevation differences between the DORIS station and all of the four grid points are below 500 m. We also rejected comparisons with too few data points or standard deviations above 0.05 m. The 702 remaining comparisons reflect a rather good agreement between DORIS and ERA-Interim data given that these use high-resolution DORIS ZTD data and 6-hourly reanalysis data.

Table 2. Statistics of Yearly DORIS Versus ERA-Interim ZTD Comparisons, for All Stations (144) and All Years (1993 to 2008), Binned as Minimum, Maximum, 5th, 50th, and 95th Percentiles[a]

	Min	5%	50%	95%	Max
	rejected = 0			used = 866	
Mean Diff. (m)	−0.0484	−0.0246	−0.0042	+0.0109	+0.0375
Std. Diff. (m)	0.0060	0.0087	0.0169	0.0330	0.0696
Corr. Coef.	+0.067	+0.677	+0.928	+0.984	+0.993
Slope	−73.00	+0.95	+1.04	+1.42	+153.33
Npoints	19	165	947	1359	1445
Selected data[b]	rejected = 164			used = 702	
Mean Diff. (m)	−0.0337	−0.0149	−0.0036	+0.0100	+0.0375
Std. Diff. (m)	0.0060	0.0087	0.0164	0.0287	0.0458
Corr. Coef.	+0.409	+0.792	+0.939	+0.985	+0.993
Slope	+0.82	+0.95	+1.03	+1.22	+1.88
Npoints	105	230	958	1338	1445

[a]The statistics are as follows: mean difference (DORIS - ERAI), standard deviation of difference, correlation coefficient, slope of linear fit (computed as ZTDDORIS = slope × ZTDERAI + offset), and the number of matched data points of the comparisons. The upper section shows results for all stations and the lower section shows results for selected stations (criteria and number of comparisons rejected and used are indicated in the header of each section). Changes in the values of at least 15% between the two sections are underlined.
[b]The rejection criteria and number of rejected stations are: $|\Delta h| > 500$ m (139 stations), Npoints < 100 (20 stations), Std.Diff. > 0.05 m (5 stations), Slope < 0.5 or > 2.5 (0 station).

3.3. Validation by Comparison With GPS ZTD Data

DORIS ZTD data were compared with GPS ZTD data from 96 colocated stations at 40 DORIS sites over the period from 1 January 1995 to 31 December 2007. Though the GPS ZTD data are not homogeneous with respect to instrumental changes either, the comparisons results show that these inconsistencies are not a limiting factor (the DORIS-GPS differences are rather dominated by DORIS ZTD errors). For more details on the GPS ZTD homogeneity the readers are referred to *Vey et al.* [2009] and *Bock et al.* [2010]. The comparisons were applied to yearly segments. After selection of comparisons with more than 100 data points, 419 yearly comparisons were available from 89 colocated stations at 39 sites. The results are reported in Table 3. The comparisons include multiple GPS stations for some DORIS stations (e.g., DORIS station GREB has five colocated GPS stations in 2007). The results show that the agreement between DORIS and GPS is slightly higher than between DORIS and ERA-Interim in the median values, especially for the standard deviation (0.0099 m compared to 0.0169 m). The results are also slightly less dispersed.

The mean statistics of the DORIS versus ERA-Interim results and DORIS versus GPS results were compared at 72 common stations, including 14 stations with a DORIS-ERA-Interim elevation difference larger than 500 m. It was found that at most stations, the ERA-Interim comparisons and the GPS comparisons were in good agreement in terms of standard deviation of differences, correlation coefficients, and slope parameters but DORIS data showed a slightly better degree of agreement with GPS data than with ERA-Interim data. This is not surprising as both space geodetic techniques use similar measurement principles based on the propagation of radio waves and have similar spatial sampling. There may also be common mode errors in the

Table 3. Similar to Table 2 but for DORIS-GPS Comparisons, for 89 Stations and All Years Available With IGS Repro1 Solution (1995 to 2007)

	Min	5%	50%	95%	Max
Selected data[a]	rejected = 16			used = 419	
Mean Diff. (m)	−0.0247	−0.0091	−0.0022	+0.0046	+0.0239
Std. Diff. (m)	0.0040	0.0056	0.0099	0.0170	0.0431
Corr. Coef.	+0.606	+0.839	+0.973	+0.994	+0.997
Slope	+0.84	+0.95	+0.99	+1.01	+1.27
Npoints	101	318	1950	4014	7980

[a]The rejection criteria and number of rejected stations are: $|h| > 500$ m (0 station), Npoints < 100 (16 stations), Std. Diff. > 0.05 m (0 station), Slope < 0.5 or > 2.5 (0 station).

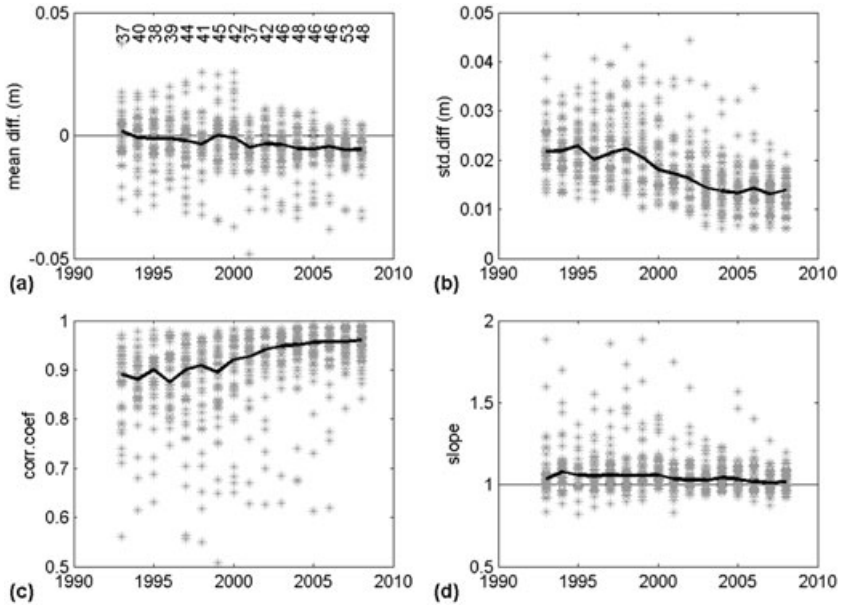

Figure 7. (a–d) Statistics of DORIS ZTD-ERA-Interim ZTD differences for 702 selected comparisons (see Table 2). The gray stars represent the yearly mean values. The black solid lines show the median over all stations. The number of stations used each year is given in Figure 7a.

space geodetic data due to the use of the same software and models (e.g., mapping function biases). Bad DORIS stations could be detected consistently from one or the other comparisons based on standard deviation of difference, slopes of linear fit, and correlations results. This consistency gives good confidence into the capacity of the ERA-Interim comparisons for detecting problems in the DORIS data, except at the sites where elevation differences are large (>500 m).

3.4. Homogenization of DORIS ZTD Data

ERA-Interim data are used to evaluate the long stability of the DORIS ZTD data. This is possible because ERA-Interim did not assimilate any DORIS data, so it is an independent data source and, though it may be possible that it contains inhomogeneity because of the inhomogeneity in the input data, it is unlikely that its inhomogeneity has similar characteristics (times and magnitudes) as that in the DORIS data.

Figure 7 shows time series of yearly mean statistics of DORIS-ERA-Interim comparisons. The agreement between DORIS and ERA-Interim improves steadily over time as revealed by decreasing standard deviation of differences, increasing correlation coefficient, and slope of linear fit approaching one. This behavior is consistent with the increase of the number of satellites and observations and with the reduction of formal error of DORIS ZTD data (Figure 2). However, the mean difference is seen to drift toward larger negative values over the period (median range: 0.0017 to −0.0057 m). This is in contrast with the findings of *Bock et al.* [2010] and of *Teke et al.* [2011] over shorter time periods. Inspection of station by station results reveals that the change of DORIS antenna from Alcatel to Starec is almost systematically accompanied with a shift of DORIS ZTD toward more negative values. Indeed, the antenna phase center offsets and variations of the two antenna types are not taken into account in the DORIS Doppler data processing software so far. A bias in the ZTD estimates is thus possible and any time variation in the antenna type or cutoff angle can result in a jump in the time series as earlier detected in GPS estimates by *Zhu et al.* [2003] after the replacement of the Block II satellites with the Block II-2A satellites. The decrease of the standard deviation of differences (Figure 7b) indicates that the Starec antennas provide ZTD estimates of higher quality.

Figure 8 shows time series of yearly mean differences separated by type of DORIS antenna. The yearly mean difference between DORIS PW and ERA-Interim PW is close to zero for the Alcatel data and negative for the Starec data. Since the antenna changes occurred progressively over the period of study (before 1999 the Alcatel antenna type was the most used, while after 1999 the Starec antenna type became dominant [*Fagard*, 2010]), the monotonic decrease of the Alcatel observations explains thus the drift toward more

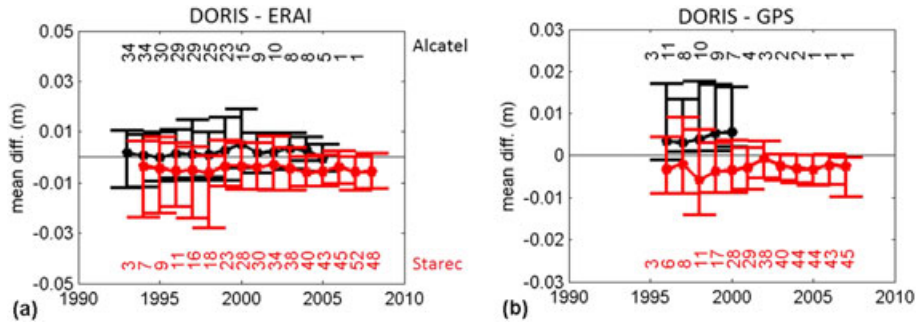

Figure 8. Statistics of ZTD comparisons for: (a) DORIS-ERA-Interim and (b) DORIS-GPS, separated by type of DORIS antenna (Alcatel in black and Starec in red). The dots indicate the median values and the error bars the 10th and 90th percentiles of the mean differences for all stations for each year. The number of stations is indicated at top and bottom of plots. Only results with at least four comparisons are plotted. The comparisons were selected indicated in Tables 2 and 3 (706 and 419 comparisons).

negative values with time in Figure 7a. The DORIS versus GPS comparison yields a similar offset between the Alcatel and Starec antennas, but the biases are more symmetric around zero (a slight positive bias is found for Alcatel data and a slight negative bias for the Starec data). The mean ± 1 standard deviation of the offsets between the median of the Alcatel bias minus the median of the Starec bias for all the sites is 0.0073 ± 0.0046 m for the DORIS-ERA-Interim comparisons and 0.0081 ± 0.0051 m for the DORIS-GPS comparisons. The mean offsets are fairly consistent between the two comparisons. We investigated if the bias could result from the fact that the DORIS positions were fixed by redoing the comparison with the DORIS solution using estimated positions (see section 2.1). Indeed, one might expect that the estimation of station position would compensate phase center offsets and hence reduce the bias in the ZTD estimates. Unfortunately, the DORIS-ERA-Interim comparison yields an offset of 0.0063 ± 0.0045 m between the two antenna types, i.e., the mean offset in the ZTD estimates is only slightly reduced A significant bias remains which might be due to phase center variations as these cannot be adjusted by the estimated parameters. A proper correction of this effect would only be obtained from the use of models determined from the calibration of the two types of DORIS antennas in anechoic chambers such as done for GPS antennas [*Schmid et al*., 2007].

For the homogenization of the present DORIS data set, biases are estimated from the DORIS vs ERA-Interim comparisons (median of the monthly mean differences) over the periods separated by events when a major equipment change is reported in the log files. The offsets are computed as the difference of the bias of a given period and the bias of the most recent period at a given site For example, site 10317 has three periods identified by three station names SPIA, SPIB, and SPJB. The correction applied to SPIA is the difference of the SPIA bias minus the SPJB bias, and the correction applied to SPIB is the difference of the SPIB bias minus the SPJB bias. In this way, we correct not only for the shifts associated with antenna changes but for all those associated with other changes such as the replacement of a beacon, relocation of the station, etc.

Figure 9 shows the offset corrections determined in this way and the standard deviation of the monthly mean differences obtained for each station pair where at least 5 months of data are available (offsets are presented for PW not ZTD in this figure). The offset corrections could be determined for 64 stations from the ERA-Interim data and for 30 common stations from the GPS data. The magnitude of the offset ranges from about 0 to about 3 kg/m^2 for Alcatel antennas and −1.5 to 1.5 kg/m^2 for Starec antennas. The GPS offsets confirm most of the ERA-Interim offsets though the GPS data may not be homogeneous themselves [*Vey et al*., 2009; *Bock et al*., 2010]. A few cases of disagreement correspond generally to stations where the altitude difference between DORIS and ERA-Interim is large, the time periods of estimation are different, or the DORIS data are noisy or contain drifts.

In addition to the station offset correction, an overall bias correction is also applied to make the homogenized DORIS data consistent with the GPS data. It consists of correcting the difference between the mean GPS and DORIS biases seen in Figure 8. Therefore, if the reference station is of Alcatel type, a bias of 0.82 kg/m^2 is subtracted and if the reference station is of Starec type, a bias of −0.47 kg/m^2 is subtracted.

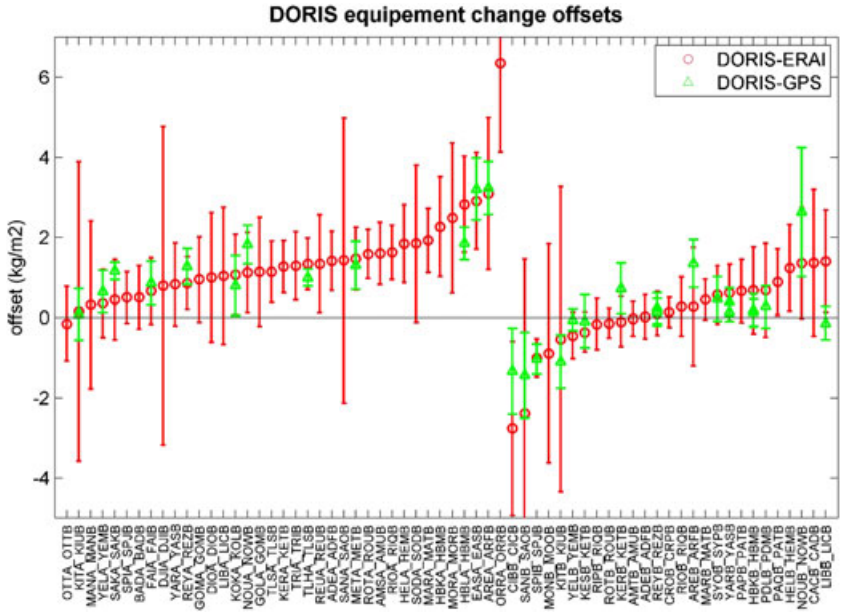

Figure 9. Estimated offsets in the DORIS PW series due to changes in equipment. The symbols show the median of the monthly mean PW differences (DORIS versus ERA-Interim as circles and DORIS versus GPS as triangles) computed for station pairs as indicated in the *x* axis label. The offsets are ordered by increasing magnitude for the sites where the antenna changed from Alcatel to Starec (left) and for the sites where other changes occurred (right).

4. Comparison of PW Data and Analysis of PW Trends

4.1. Comparison of PW Data

The high-resolution homogenized DORIS PW data are compared with PW data from ERA-Interim, GPS, radiosondes, and satellites. Figure 10 shows the histograms of mean difference, standard deviation of the differences, correlation coefficient, and slope of linear fit for all four comparisons. The comparisons only include DORIS stations with altitude difference with the other instruments $<$100 m and altitude difference with ERA-Interim $<$500 m (the latter constraint guarantees that accurate surface pressure from ERA-Interim is used for the conversion of DORIS ZTD to IWV, see section 2.6). Table 4 reports the median values of the histograms.

The most striking result in Figure 10 is the very good agreement between DORIS and GPS PW data, which was already found from the ZTD comparison (section 3.3). The second best agreement is found between DORIS and satellites, though the statistics displayed here are redundant because they include multiple DORIS comparisons with different satellites (only 20 DORIS stations at 12 sites are used). The standard deviations of the differences and correlation coefficients indicate that the DORIS and satellite times series measure consistent high-resolution PW variations. The DORIS and ERA-Interim PW data also show good agreement, very similar to those obtained from the satellite comparison, though these two data sets are not completely independent since DORIS data were screened and homogenized using ERA-Interim data. Finally, the radiosonde comparison shows the poorest results, with a broad scatter in the mean and standard deviation of differences, and reduced correlation coefficients. This poor agreement might be due to sampling differences produced by the drift of the balloons combined with the fact that most stations in the comparison are on islands or near the coast where water vapor variability is high. The peak in the slope of linear fit parameters $<$ 1 suggests that the 10% uncertainty associated to these data may be too small. The histograms for the radiosonde comparison show several secondary peaks which suggest that the radiosonde data set is not spatially homogeneous [*Wang et al.*, 2013].

Figure 11 shows the time series of monthly PW differences at three DORIS sites with and without homogenized DORIS PW data. The monthly values were computed from at least 10 high-resolution values in the case of the DORIS versus radiosonde and satellite data comparisons and 50 values in the case of DORIS versus GPS and ERA-Interim comparisons. At DORIS site 10317 (Ny Alesund, Norway) the shifts in the

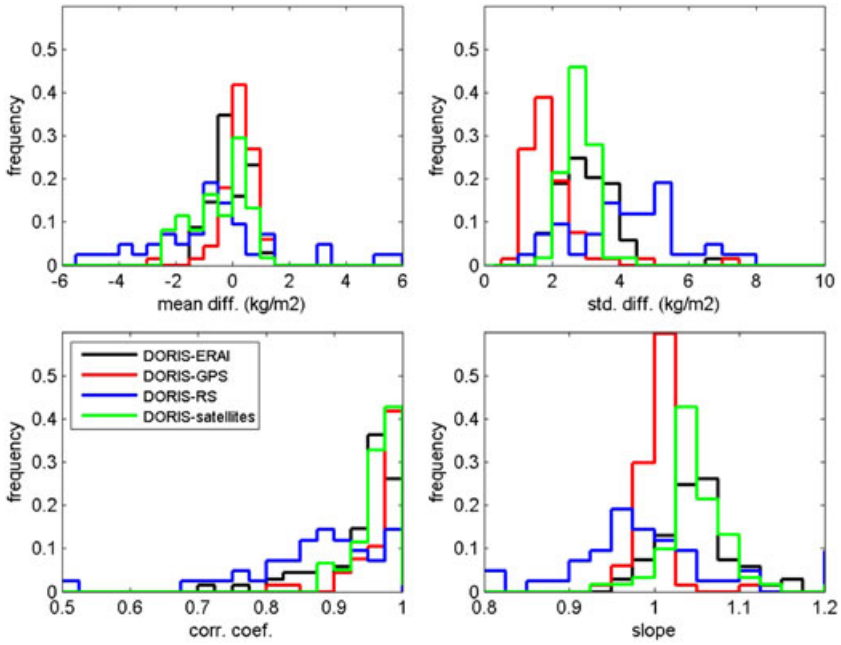

Figure 10. Histograms of PW comparisons of DORIS versus ERA-Interim, GPS, radiosondes, and satellites (SSMI, SSMIS, and AMSR-E). The histograms are computed over the full time series for data pairs with at least 20 matched points and instruments with altitude differences smaller than 100 m. The DORIS PW data are converted from ZTD when the altitude difference with ERA-Interim grid points is smaller than 500 m. In the case of the satellite results, multiple comparisons are included when several satellites are available for a given DORIS station.

biases are well captured by all three comparisons (DORIS versus ERA-Interim, GPS, and radiosonde). Surprisingly, the bias is the largest for the central period (SPIB) and not for the period when an Alcatel antenna was used (SPIA). The homogenization properly removes the shifts from one period to another one. At DORIS site 41703 (Eastern Island, Chile), the large shift between EASA and EASB is consistently detected from ERA-Interim, GPS, and SSMI comparisons, but not from the radiosonde comparison which shows very large scatter in the PW differences. The shift is well removed with the homogenization procedure. At DORIS site 92701 (Noumea, New-Caledonia, France), a shift between NOUA and NOWB is properly corrected according to the comparisons with ERA-Interim and GPS, but the NOUB station has a too short period with a large scatter which cannot be reduced accurately. Also, at this site we see several shifts in the DORIS versus radiosonde comparison, which are explained by the following changes in sonde types: Vaisala RS80 before January 2002, Vaisala RS90 between January 2002 and February 2005 and Modem M2K2 between February 2005 and March 2008 and Modem M2K2-DC after March 2008 (T. Bourcy, Meteo-France, personal communication, 2013).

Table 4. Statistics of PW Comparisons of DORIS Verus ERA-Interim, GPS, Radiosondes, and Satellites (SSMI, SSMIS, and AMSR-E)[a]

	Mean Diff. (kg/m2)	Std. Diff. (kg/m2)	Corr. Coef.	Slope	Nsta used
DORIS-ERAI	−0.43	2.70	0.951	1.038	69
DORIS-GPS	0	1.47	0.979	0.991	67
DORIS-RS	−0.84	4.12	0.867	0.974	44
DORIS-satellite	−0.47	2.51	0.961	1.029	61

[a]The statistics are computed over the full time series for data pairs with at least 20 matched points and instruments with altitude differences smaller than 100 m. The DORIS PW data are converted from ZTD when the altitude difference with ERA-Interim grid points is smaller than 500 m. The Table reports medians values computed over the results from the ensemble of stations (the number of used stations is indicated in the last column). In the case of the satellite results, multiple comparisons are included when several satellites are available for a given DORIS station.

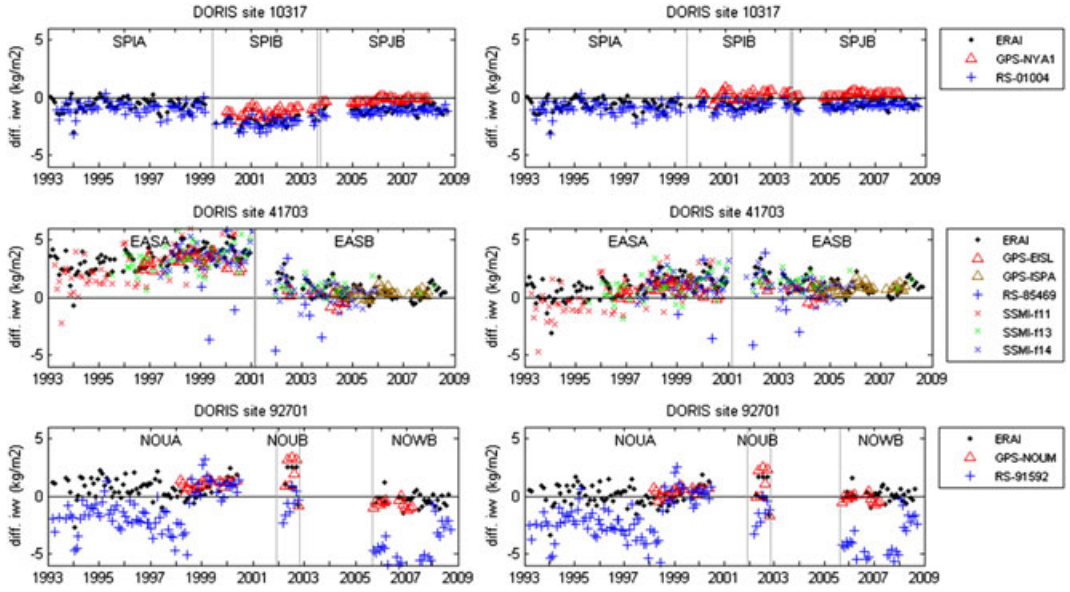

Figure 11. Time series of monthly PW differences at three DORIS sites (left) before and (right) after bias offset correction with respect to the most recent period from DORIS versus ERAI comparisons (offsets are shown in Figure 9).

4.2. Analysis of PW Trends and Variability

The time series of monthly PW data are analyzed using a linear trend + harmonic model following *Weatherhead et al.* [1998]: $Y_t = \mu + \omega X_t + S_t + N_t$, where μ is a constant term, ωX_t represents the linear trend function (X_t is time and ω is the magnitude of the trend), S_t is a seasonal component modeled by the first four terms of a Fourier series: $S_t = \sum_{j=1}^{4}\left[\beta_{1,j}\sin(2\pi jt) + \beta_{2,j}\cos(2\pi jt)\right]$, and N_t is the noise in the data. The

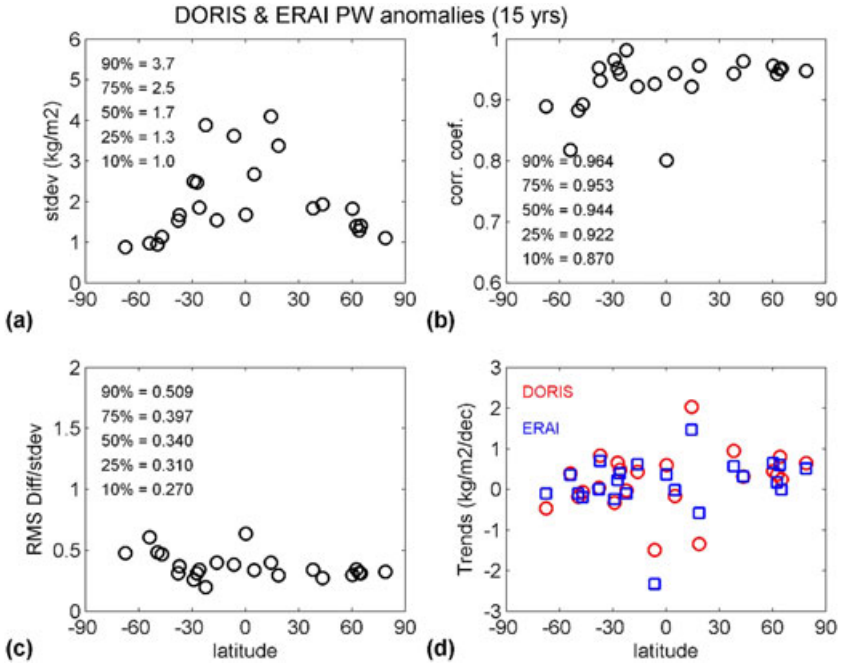

Figure 12. Analysis of PW anomalies from DORIS and ERA-Interim with more than 15 years of matched data (23 sites): (a) standard deviation of monthly PW anomalies (average between DORIS and ERAI), (b) correlation coefficient, (c) ratio of the RMS difference to the standard deviation, and (d) linear trends. Percentiles are given in each panel except in Figure 12d. Each dot represents one DORIS site.

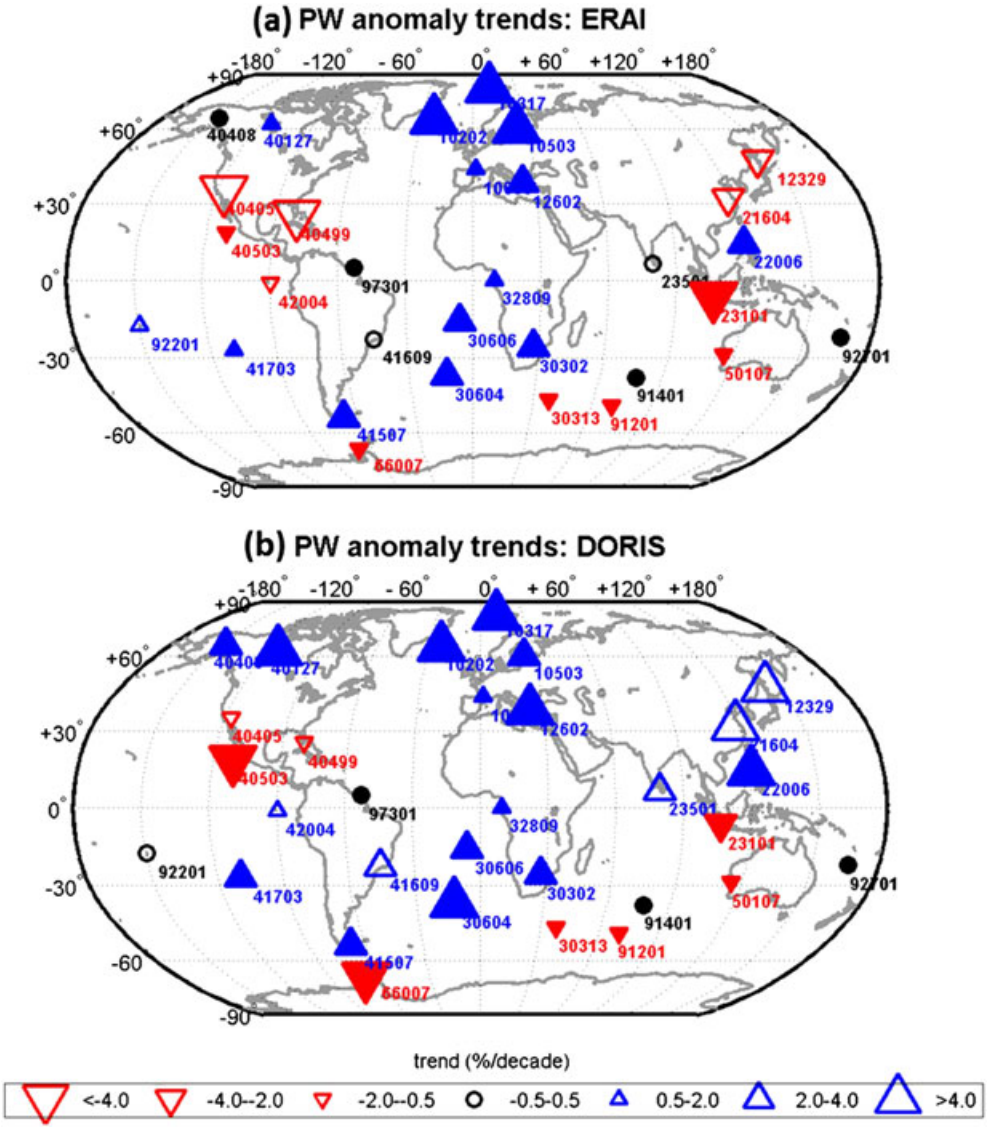

Figure 13. Spatial distribution of the linear trends estimated from matched DORIS and ERA-Interim PW data in percent per decade. The open symbols are for time series of less than 15 years but more than 10 years, and the filled symbols are for time series of more than 15 years. The trend errors range from 0.16 to 0.22 kg m^{-2} per decade.

parameters of the model (μ, ω, $\beta_{1,j}$, and $\beta_{2,j}$, $j = 1..4$) and their uncertainties are estimated by a least squares method. The PW anomalies are computed as $Y_t - \mu - S_t = \omega X_t + N_t$. The matched DORIS and ERA-Interim PW data provide trend estimates at 31 sites with more than 10 years and less than 15 years of data and at 23 sites with more than 15 years of data (for both periods we used only stations for which the data were available for at least half of the months). PW anomalies are computed as the monthly PW series minus the series modeled with the above linear trend + harmonic model. The trends and variability are shown in Figure 12 as a function of latitude. The standard deviation of PW anomalies show a peak of variability around the equator (~4 kg m^{-2}) and a minimum near the poles (~1 kg m^{-2}). The correlation coefficients and normalized RMS differences reveal that the variability contained in both data sets is highly consistent. The estimated trends range globally from −2.5 to +1.0 kg m^{-2} per decade for the 15 year data set. Figure 12d shows that the DORIS and ERA-Interim trends are in good agreement (they correlate to 90% and the standard deviation of their difference is 0.3 kg m^{-2} per decade). Similar agreement between model and observations was found by *Trenberth et al.* [2005] who analyzed radiosonde data and ERA40 data for the 1973–1995 period in the Northern Hemisphere (see their Figure 2).

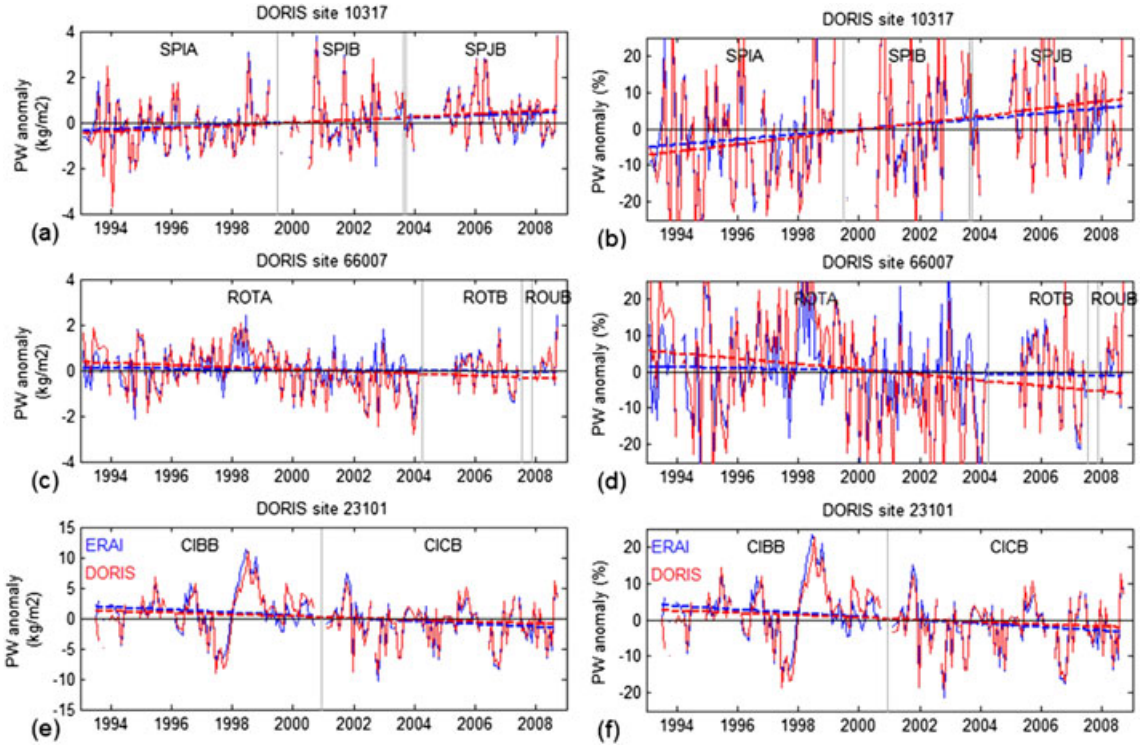

Figure 14. Time series of monthly PW anomaly (a, c, and e) in kg m-2 and (b, d, and f) in %, with fitted trends (thick dashed lines) from ERA-Interim (blue) and DORIS (red) at three sites: Ny-Ålesund, Norway is shown in Figures 14a and 14b, Rothera, Antarctica is shown in Figures 14c and 14d, and Cibinong, Indonesia is shown in 14e and 14f. Note the change in vertical scale between the polar sites as shown in Figures 14a and 14c and the tropical site Figures 14e.

Figure 13 shows the spatial distribution of the linear trends estimated from matched DORIS and ERA-Interim PW data. There is high consistency between the trends estimated from both data sets at most regions with a few exceptions. If we focus on the 15 year data set, we can notice consistent and large positive trends in the 30°W–30°E zone in both hemispheres, though very few sites are available over continental Africa. The trends at the coastal sites in the U.S. are negative while the trends north of 45°N on the North American continent are positive. Trends at Rothera, Antarctica (DORIS site 66007) and four other sites in the Indian Ocean are also negative. There is thus high consistency in the signs of the estimated trends from the two 15 year data sets but there are some differences in the magnitudes. The trend errors estimated from the least squares fit (assuming uncorrelated errors in the data) range from 0.16 to 0.22 kg m^{-2} per decade (10th and 90th percentiles) with a rather uniform latitudinal distribution. Due to lower PW near the poles, the trend errors when expressed in percent per decade increase from 0.3 at the equator to 3.0% per decade at the poles. The few sites with less than 15 years but more than 10 years of data show less consistent trends and in some occasions trends of opposite signs are found. For example, the trends over eastern Asia and northern Canada estimated from DORIS and ERA-Interim data are not consistent. Overall, our results contrast with those of *Trenberth et al*. [2005] but are rather fairly consistent with those of *Mieruch et al*. [2008] who used satellite data in visible spectral range for 1996–2006. Indeed, it is difficult to derive a general picture for the global PW trends from a sparse network such as DORIS. Nevertheless, the DORIS PW trends are highly valuable for validating model outputs and satellite products from which a two-dimensional analysis is possible. Also, trends estimated at nearby sites but over short or different periods can be inconsistent. An example was found for DORIS sites 92901 and 92902 (13°S, 176°W) which are located on two islands of the Wallis and Futuna French territory in the Pacific Ocean about ~250 km apart (these sites have less than 10 years of data and are not shown in Figure 13). The signs of the trends at these two sites are opposite but DORIS and ERA-Interim estimates are consistent. This example suggests that trends estimated from station data can vary substantially over very short distances and short periods of time. One should also mention that given the short record (15 years) the trends are very sensitive to interannual variability and starting/ending values.

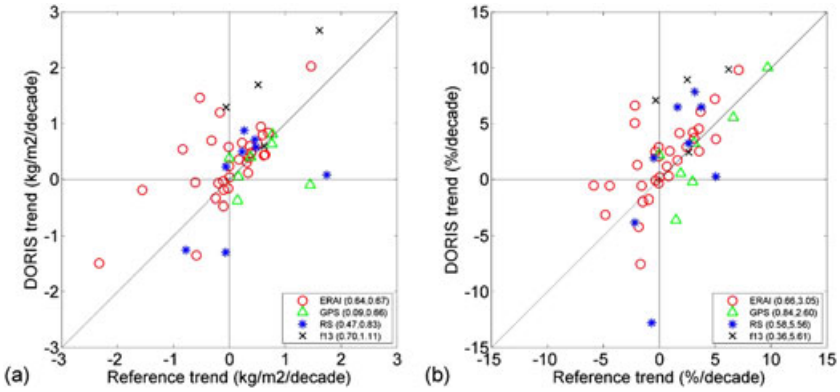

Figure 15. Scatterplot of PW anomaly trends estimated from DORIS and the reference data sets with at least 10 years of data: (a) trends in kg m^{-2} per decade and (b) trends in percent per decade. Each dot represents a pair of trend estimates computed from matched DORIS and reference data. The numbers in the legend give the linear correlation coefficients and the RMS difference in the same unit as the trends. The ERA-Interim comparison counts 31 sites, GPS counts 7 sites, radiosonde 8 sites, and f13 (SSM/I) 4 sites.

Figure 14 illustrates the PW anomalies at two polar sites (Ny-Ålesund, Norway, and Rothera, Antarctica) and one tropical site (Cibinong, Indonesia) with large positive or negative trends. At all three sites, the PW anomalies show large variability but the DORIS and ERA-Interim time series are in excellent agreement. The variations are high frequency and exceed ± 2 kg m^{-2} (±20%) at both polar sites. The tropical site shows smoother variations but a large oscillation of ± 10 kg m^{-2} (±20%) can be seen which is linked to the 1997–1998 El Niño event. The large positive trend at Ny-Ålesund and the large negative trend at Cibinong are consistent between both data sets but at Rothera the negative trend seen in the DORIS data (−0.47 kg m^{-2} or −7.5% per decade) is much larger than the one estimated from ERA-Interim (−0.11 kg m^{-2} or −1.7% per decade). No other data were available at that site to examine which of both is correct, but DORIS and GPS data available at another station in Antarctica (Syowa) reveal a similar large negative trend (−0.28 kg m^{-2} or −7.8% per decade). The strong positive trends over Europe and Canada are also confirmed from GPS data.

Figure 15 compares the DORIS PW anomaly trends to the trends estimated from the four reference data sets with at least 10 years of data. Few sites are available in this comparison and the statistics should be regarded with precaution. DORIS and ERA-Interim show a linear correlation coefficient of 0.64–0.66 and a RMS difference of 0.67 kg m^{-2} per decade (3.0% per decade). The consistency between DORIS and ERA-Interim is very good but these two data sets are not completely independent since ERA-Interim PW is used to homogenize the DORIS data. The correlation between DORIS and GPS trends is bad in units of kg m^{-2} per decade mainly because of a discrepancy at two sites where the problems seem attributable to the GPS data, namely a change in equipment at station KERG and a drift in the PW time series at station KRUG, and at one site (HBLA) where the offset in the DORIS time series is badly corrected due to a spurious annual signal in the ERA-Interim data. In units of percent per decade, the correlation between DORIS and GPS improves to 0.84 because the mean PW is high at the sites where a large discrepancy was observed. The radiosonde and satellite comparisons show less good agreement on average. The radiosonde comparison contains two outliers far from the 1:1 line. One is the case of DORIS site 92701 where the radiosonde time series contains large scatter and discontinuities as shown in Figure 12. For the other problematic radiosonde and satellite comparisons, it seems that the DORIS data systematically overestimate the PW anomaly trends, though the same DORIS data are generally fairly consistent with the ERA-Interim and the GPS trends. This seems to be a result of the undersampling of the time series combined with the fact that the DORIS bias is not constant at these stations but contains linear and nonlinear time variations (e.g., DORIS site 41703 on Figure 12).

5. Summary and Conclusions

This is the first time that long time series of reprocessed DORIS ZTD and PW data are analyzed. We have developed a method for screening the DORIS ZTD estimates based on a two-level procedure. The first level uses DORIS postprocessing information and applies range checks and outlier checks on ZTD and formal error estimates. Since the number of satellites has increased over time, and the quality of the DORIS data

varies from site to site, the screening is performed independently for each station and each year using matched thresholds. This screening is effective and rejects about 3% of the data. The second level is based on the comparison of DORIS ZTD and a reference ZTD data set for which we used the ERA-Interim reanalysis. This is a more physical check of the ZTD data compared to the first screening level which is primarily based on statistics of the formal errors. A global reanalysis such as ERA-Interim provides a continuous reference which is available for all the stations and all the time. However, due to its limited horizontal resolution (0.75° by 0.75°), we found representativeness differences at some sites which introduce biases and scatter in the ZTD differences consistently with *Bock and Nuret* [2009]. However, the comparison to the reanalysis is nevertheless effective in detecting shifts in the DORIS ZTD data due to changes in equipment or relocation of the stations. A major source of inhomogeneity in the DORIS ZTD time series was evidenced which is due to antenna changes. It affects all the sites and produces offsets of 0–3 kg m^{-2}. Other sources of inhomogeneity are relocation of the antennas and other equipment changes which produce offsets of ± 1.5 kg m^{-2}. The DORIS ZTD and PW time series were thus homogenized and validated with GPS comparisons. The homogenization was based on the estimation of constant offsets between documented discontinuities (indicated by changes of DORIS station name). These screening and homogenization methods can be easily applied to any future release of reprocessed DORIS data.

The DORIS ZTD data were converted to PW using bilinearly interpolated surface pressure from ERA-Interim and mean temperature from ECMWF analyses. Though these supporting information may not be perfect, they represent the best estimate we can have for these parameters since only sparse, discontinuous, and often uncalibrated meteorological measurements are available at these sites. In order to limit the errors introduced by the PW conversion, we restricted the PW data set to sites where the elevation difference with the four surrounding model grid points are smaller than 500 m. The homogenized DORIS PW data set was compared with four PW data sets (ERA-Interim, GPS, radiosondes, and microwave radiometer satellites). The DORIS PW is shown to be in very good agreement with these data sets (a correlation of 0.98 and a standard deviation of differences of 1.5 kg m^{-2} with GPS data, and a correlation $>$ 0.95 and a standard deviation of differences $<$ 2.7 kg m^{-2} with ERA-Interim and satellite PW data), reaching nearly similar performance as the GPS PW data sets analyzed in previous studies [*Wang et al*., 2007; *Bock and Nuret*, 2009; *Vey et al*., 2009]. Preliminary trends and variability were analyzed from monthly PW data at 31 sites with more than 10 years of measurements and 23 sites with more than 15 years of measurements. It is shown that DORIS PW data and ERA-Interim data are generally in good agreement though these two data sets are not completely independent since DORIS data were screened and homogenized using ERA-Interim data. A few examples are shown which highlight that DORIS is capable of detecting the contrasted seasonal cycles, anomalies and trends both in the very dry polar climates and in the very wet intertropical climates.

The perspectives of this work are twofold. First, the present data set will be used for the study of water vapor trends and variability on global scale in complement to other PW data sets (GPS, radiosonde, and satellites) and to climate model simulations which the observational data sets will help validating. Model validation is of special importance in regions such as the tropics and the monsoon regions, but also in the Polar Regions, where model uncertainties are high. The DORIS PW data set may also be useful for the validation and the homogenization of radiosonde data and satellite data over the past 20 years. It can be envisioned that the ground-based DORIS and GPS networks will contribute to the Network for the Detection of Atmospheric Composition Change and the World Meteorological Organization Global Climate Observing System Reference Upper-Air Network in the near future as complementary long-term monitoring systems and reference systems for the measurement of water vapor [*Immler et al*., 2010]. Second, methodological studies will be conducted and a new improved and extended (from 1990 to present) data set will be produced. A major improvement might result from the introduction of antenna phase center offset and variation models as planned by IDS in the near future. We expect that reprocessed DORIS data using such models will be less impacted by antennas changes and less sensitive to elevation cutoff angle, and also possibly provide improved absolute accuracy in the ZTD estimates. However, in parallel, we will also study more sophisticated homogenization methods to detect undocumented discontinuities and account for non-constant biases.

The data set developed in this work is freely available in the supporting information. We encourage other researchers to use this data set for their research. Future releases will be made available to the scientific community through a dedicated web site.

Acknowledgments
This work was supported by the Centre National d'Etudes Spatiales (CNES). It is based on observations with DORIS embarked on SPOT satellites, TOPEX/Poseidon, ENVISAT, Jason-2, and Cryosat-2 satellites. The ERA-Interim data were provided by IPSL/CNRS and are available on the "climserv" database. The GPS tropospheric solution was provided by JPL and is publicly available on the IGS database. The authors would like to acknowledge Yoaz Bar Sever and Sun Buyn, JPL/NASA, for providing details on the GPS data processing at JPL.

References

Altamimi, Z., X. Collilieux, and L. Metivier (2011), ITRF2008, An improved solution of the International Terrestrial Reference Frame, *J. Geod.*, *85*(8), 457–473.

Auriol, A., and C. Tourain (2010), DORIS system: The new age, *Adv. Space Res.*, *46*(12), 1484–1496.

Bock, O., and M. Nuret (2009), Verification of radiosonde humidity data and NWP model analyses and forecasts during AMMA with GPS precipitable water estimates, *Weather Forecasting*, *24*, 1085–1101, doi:10.1175/2009WAF2222239.1.

Bock, O., M.-N. Bouin, A. Walpersdorf, J.-P. Lafore, S. Janicot, F. Guichard, and A. Agusti-Panareda (2007), Comparison of ground-based GPS precipitable water vapour to independent observations and numerical weather prediction model reanalyses over Africa, *Q. J. R. Meteorol. Soc.*, *133*, 2011–2027, doi:10.1002/qj.185.

Bock, O., et al. (2008), The West African Monsoon observed with ground-based GPS receivers during AMMA, *J. Geophys. Res.*, *113*, D21105, doi:10.1029/2008JD010327.

Bock, O., P. Willis, M. Lacarra, and P. Bosser (2010), An inter-comparison of zenith tropospheric delays derived from DORIS and GPS data, *Adv. Space Res.*, *46*(12), 1648–1660, doi:10.1016/j.asr.2010.05.018.

Bock, O., et al. (2013), Accuracy assessment of water vapour measurements from in-situ and remote sensing techniques during the DEMEVAP 2011 campaign at OHP, *Atmos. Meas. Tech.*, *6*, 2777–2802, doi:10.5194/amt-6-2777-2013.

Boehm, J., A. E. Niell, P. Tregoning, and H. Schuh (2006), The Global Mapping Function (GMF): A new empirical mapping function based on numerical weather model data, *Geophys. Res. Lett.*, *33*, L07304, doi:10.1029/2005GL025546.

Byun, S. H., and Y. E. Bar-Server (2009), A new type of troposphere zenith path delay product of the international GNSS service, *J. Geod.*, *83*(3-4), 367–373, doi:10.1007/s00190-008-0288-8.

Dai, A., J. Wang, P. W. Thorne, D. E. Parker, L. Haimberger, and X. L. Wang (2011), A new approach to homogenize daily radiosonde humidity data, *J. Clim.*, *24*, 965–991.

Dow, J., R. E. Neilan, and C. Rizos (2009), The International GNSS Service in a changing landscape of Global Navigation Satellite Systems, *J. Geod.*, *83*(3–4), 191–198.

Fagard, H. (2010), Twenty years if evolutions of the DORIS permanent network: From its initial deployment to its renovation, *J. Geod.*, *80*(8-11), 429–456.

Ferland, R., and M. Piraszewski (2009), The IGS-combined station coordinates, earth rotation parameters and apparent geocenter, *J. Geod.*, *83*(3-4), 385–392.

Ferrage, P., A. Auriol, C. Tourain, C. Jayles, and F. Boldo (2012), DORIS system developments and future missions, IDS Workshop, Venice, Italy, 25–26 September. [Available at http://ids-doris.org/images/documents/report/ids_workshop_2012/IDS12_s1_Auriol_DORISstatus.pdf.]

Gobinddass, M. L., P. Willis, A. Sibthorpe, N. P. Zelensky, F. G. Lemoine, J. C. Ries, R. Ferland, Y. E. Bar-Sever, O. de Viron, and M. Diament (2009), Improving DORIS geocenter time series using an empirical rescaling of solar radiation pressure models, *Adv. Space Res.*, *44*(11), 1279–1287, doi:10.1016/j.asr.2009.08.004.

Gobinddass, M. L., P. Willis, M. Menvielle, and M. Diament (2010), Refining DORIS atmospheric drag estimation in preparation of ITRF2008, *Adv. Space Res.*, *46*(12), 1566–1577, doi:10.1016/j.asr.2010.04.004.

Held, I. M., and B. J. Soden (2000), Water vapor feedback and global warming, *Annu. Rev. Energy Env.*, *25*, 445–475.

IGSMAIL-6298 (2012), Reprocessed IGS Trop Product now available with Gradients, by Yoaz Bar-Sever, 11 November. [Available at http://igscb.jpl.nasa.gov/pipermail/igsmail/2010/007488.html.]

Immler, F. J., J. Dykema, T. Gardiner, D. N. Whiteman, P. W. Thorne, and H. Vömel (2010), A guide for upper-air reference measurements: Guidance for developing GRUAN data products, *Atmos. Meas. Tech. Discuss.*, *3*, 1217–1231, doi:10.5194/amt-3-1217-2010.

Jayles, C., J. P. Chauveau, and F. Rozo (2010), DORIS/Jason-2: Better than 10 CM On-Board orbits available for Near-Real-Time Altimetry, *Adv. Space Res.*, *46*(12), 1497–1512, doi:10.1016/j.asr.2010.04.030.

Le Bail, K., F. G. Lemoine, and D. S. Chinn (2010), GSFC contribution to ITRF2008, *Adv. Space Res.*, *45*(12), 1481–1499, doi:10.1016/j.asr.2010.01.030.

Lemoine, F. G., et al. (2010), Towards development of a consistent orbit series for TOPEX, Jason-1, and Jason-2, *Adv. Space Res.*, *46*(12), 1513–1540, doi:10.1016/j.asr.2010.05.007.

Lindstrot, R., M. Stengel, M. Schröder, J. Fischer, R. Preusker, N. Schneider, and T. Steenbergen (2014), A global climatology of total columnar water vapour from SSM/I and MERIS, *Earth Syst. Sci. Data Discuss.*, *7*, 59–88, doi:10.5194/essdd-7-59-2014.

Mears, C. A., B. D. Santer, F. J. Wentz, K. E. Taylor, and M. F. Wehner (2007), Relationship between temperature and precipitable water changes over tropical oceans, *Geophys. Res. Lett.*, *34*, L24709, doi:10.1029/2007GL031936.

Mieruch, S., S. Noël, H. Bovensmann, and J. P. Burrows (2008), Analysis of global water vapour trends from satellite measurements in the visible spectral range, *Atmos. Chem. Phys.*, *8*, 491–504, doi:10.5194/acp-8-491-2008.

Nilsson, T., and G. Elgered (2008), Long-term trends in the atmospheric water vapor content estimated from ground-based GPS data, *J. Geophys. Res.*, *113*, D19101, doi:10.1029/2008JD010110.

Ning, T., and G. Elgered (2012), Trends in the atmospheric water vapor content from ground-based GPS: The impact of the elevation cutoff angle, *IEEE J. Sel. Top. Appl. Earth Obs. Remote Sens.*, *5*, 744–751, doi:10.1109/JSTARS.2012.2191392.

Ning, T., G. Elgered, U. Willén, and J. M. Johansson (2013), Evaluation of the atmospheric water vapor content in a regional climate model using ground-based GPS measurements, *J. Geophys. Res. Atmos.*, *118*, 329–339, doi:10.1029/2012JD018053.

Ross, R. J., and W. P. Elliott (2001), Radiosonde-based Northern Hemisphere tropospheric water vapor trends, *J. Clim.*, *14*, 1602–1611.

Schmid, R., P. Steigenberger, G. Gendt, M. Ge, and M. Rothacher (2007), Generation of a consistent absolute phase center correction model for GPS receiver and satellite antennas, *J. Geod*, *81*, 781–798, doi:10.1007/s00190-007-0148-y.

Shi, L., and J. J. Bates (2011), Three decades of intersatellite-calibrated High-Resolution Infrared Radiation Sounder upper tropospheric water vapor, *J. Geophys. Res.*, *116*, D04108, doi:10.1029/2010JD014847.

Simmons, A., S. Uppala, D. Dee, and S. Kobayashi (2006), ERA-Interim: New ECMWF reanalysis products from 1989 onwards, Newsletter 110 - Winter 2006/07, ECMWF, 11 pp.

Solomon, S., D. Qin, M. Manning, Z. Chen, M. Marquis, K. B. Averyt, M. Tignor, and H. L. Miller (Eds.) (2007), *Contribution of Working Group I to the Fourth Assessment Report of the Intergovernmental Panel on Climate Change (2007)*, Cambridge Univ. Press, Cambridge, U. K., and New York.

Stepanek, P., V. Filler, U. Hugentobler, and J. Dousa (2010), DORIS at GOP: From pilot testing campaign to fully operational analysis center, *Acta Geodyn. Geomater.*, *7*(1), 49–60.

Tavernier, G., L. Soudarin, K. Larson, C. Noll, J. Ries, and P. Willis (2002), Current status of the DORIS Pilot Experiment and the future international DORIS Service, *Adv. Space Res.*, *30*(2), 151–156, doi:10.1016/s0273-1177(02)00279-x.

Teke, K., et al. (2011), Multi-technique comparison of troposphere zenith delay and gradients during CONT08, *J. Geod.*, *85*(7), 395–413, doi:10.1007/s00190-010-0434-y.

Trenberth, K. E., J. Fasullo, and L. Smith (2005), Trends and variability in column integrated atmospheric water vapor, *Clim. Dyn.*, *24*(7–8), 741–758.

Vey, S., R. Dietrich, M. Fritsche, A. Rülke, P. Steigenberger, and M. Rothacher (2009), On the homogeneity and interpretation of precipitable water time series derived from global GPS observations, *J. Geophys. Res.*, *114*, D10101, doi:10.1029/2008JD010415.

Wang, J., and L. Zhang (2008), Systematic errors in global radiosonde precipitable water data from comparisons with ground-based GPS measurements, *J. Clim.*, *21*, 2218–2238, doi:10.1175/2007JCLI1944.1.

Wang, J., and L. Zhang (2009), Climate applications of a global, 2-hourly atmospheric precipitable water dataset derived from IGS tropospheric products, *J. Geod.*, *83*, 209–217, doi:10.1007/s00190-008-0238-5.

Wang, J., H. L. Cole, and D. J. Carlson (2001), Water vapor variability in the tropical western Pacific from a 20-year radiosonde data, *Adv. Atmos. Sci.*, *18*, 752–766.

Wang, J., L. Zhang, A. Dai, T. Van Hove, and J. Van Baelen (2007), A near-global, 2-hourly data set of atmospheric precipitable water from ground-based GPS measurements, *J. Geophys. Res.*, *112*, D11107, doi:10.1029/2006JD007529.

Wang, J., L. Zhang, A. Dai, F. Immler, M. Sommer, and H. Vömel (2013), Radiation Dry bias correction of Vaisala RS92 humidity data and its impacts on historical radiosonde data, *J. Atmos. Oceanic Technol.*, *30*, 197–214, doi:10.1175/JTECH-D-12-00113.1.

Weatherhead, E. C., et al. (1998), Factors affecting the detection of trends: Statistical considerations and applications to environmental data, *J. Geophys. Res.*, *103*(D14), 17,149–17,161, doi:10.1029/98JD00995.

Wentz, F. J. (2013), SSM/I Version-7 Calibration Report, report number 011012, Remote Sensing Systems, 46 pp., Santa Rosa, Calif.

Williams, S. D. P., and P. Willis (2006), Error analysis of weekly station coordinates in the DORIS network, *J. Geod.*, *80*(8-11), 525–539, doi:10.1007/s00190-006-0056-6.

Willis, P., and J. C. Ries (2005), Defining a DORIS core network for Jason-1 precise orbit determination, methods and realization, *J. Geod.*, *79*(6-7), 370–378.

Willis, P., C. Jayles, and Y. E. Bar-Sever (2006), DORIS, from altimetric missions orbit determination to geodesy, *C. R. Geosci.*, *338*(14-15), 968–979.

Willis, P., J. C. Ries, N. P. Zelensky, L. Soudarin, H. Fagard, E. C. Pavlis, and F. G. Lemoine (2009), DPOD2005: An extension of ITRF2005 for Precise Orbit Determination, *Adv. Space Res.*, *44*(5), 535–544, doi:10.1016/j.asr.2009.04.018.

Willis, P., C. Boucher, H. Fagard, B. Garayt, and M. L. Gobinddass (2010a), Contributions of the French Institut Geographique National (IGN) to the International DORIS Service, *Adv. Space Res.*, *45*(12), 1470–1480, doi:10.1016/j.asr.2009.09.019.

Willis, P., et al. (2010b), The International DORIS Service. Toward maturity, *Adv. Space Res.*, *45*(12), 1408–1420, doi:10.1016/j.asr.2009.11.018.

Willis, P., Y. E. Bar-Sever, and O. Bock (2012a), Estimating horizontal tropospheric gradients in DORIS data processing: Preliminary results, *IAG Symp.*, *136*, 1013–1019, doi:10.1007/978-3-642-20338-1_127.

Willis, P., M.-L. Gobinddass, B. Garayt, and H. Fagard (2012b), Recent improvements in DORIS data processing in view of ITRF2008, the ignwd08 solution, *IAG Symp.*, *136*, 43–49, doi:10.1007/978-3-642-20338-1_6.

York, D., N. Evensen, M. Martinez, and J. Delgado (2004), Unified equations for the slope, intercept, and standard errors of the best straight line, *Am. J. Phys.*, *72*, 367–375.

Zhu, S. Y., F. H. Massmann, Y. Yu, and C. Reigber (2003), Satellite antenna phase center offsets and scale errors in GPS solutions, *J. Geod.*, *76*(11-12), 668–672.

Zumberge, J. F., M. B. Heflin, D. C. Jefferson, M. M. Watkins, and F. H. Webb (1997), Precise point positioning for the efficient and robust analysis of GPS data from large networks, *J. Geophys. Res.*, *102*(B3), 5005–5017, doi:10.1029/96JB03860.